Influence surfaces for bending moments in circular cylindrical shells or curved plates

Autor(en): **Holand, Ivar**

Objekttyp: **Article**

Zeitschrift: **IABSE publications = Mémoires AIPC = IVBH Abhandlungen**

Band (Jahr): **21 (1961)**

PDF erstellt am: **10.07.2024**

Persistenter Link: https://doi.org/10.5169/seals-18249

Influence Surfaces for Bending Moments in Circular Cylindrical Shells or Curved Plates

Surfaces d'influence pour les moments de flexion des voiles cylindriques ou des plaques incurvées

Momenteneinflußflächen von kreiszylindrischen Schalen oder gekrümmten Platten

IVAR HOLAND
Dr. techn., The Technical University of Norway, Trondheim

Introduction

In the last two decades influence surface diagrams have found extensive use for calculating bending moments in plates loaded with concentrated loads. Numerous charts for rectangular plates are given by PUCHER [1] and by GÜNTER HOELAND [2] and for circular plates by PERSEN [3].

The very first influence surface diagram for a cylindrical shell was probably given by YUAN [4], but charts of real practical use were not given till the thesis of BIEGER [5] appeared.

The approaches known to the writer, which have been used for analyzing the influence of concentrated loads on shells, may be arranged in three groups. As was shown originally by H. REISSNER [6], any kind of loading on a simply supported cylindrical shell may be treated by developing the load in a double trigonometric series. This method has been used by BIJLAARD [7, 8] for calculating moments and forces under rectangular loads. The method has the advantage of giving a simple expression for the general series term, but the series converges very slowly. An effective way of improving the convergence, shown by WLASSOW [9], is to subtract the series solution for the corresponding plate problem and calculate the plate quantities by other methods.

A second group of methods result in a single Fourier series with trigonometric functions in the circumferential direction and damped trigonometric functions longitudinally. A solution in this form is obtained if the load is

considered an edge disturbance from a section through the load point and normal to the axis (used by ERNST [10] and KOEPCKE [11] and for a load on a rib by LUNDGREN [12]). Alternatively a solution in the same form may be obtained by representing the concentrated load by a Fourier series circumferentially and a Fourier integral longitudinally (used by YUAN [4], YUAN and TING [13, 14], BIEGER [5], and MORLEY [15]). A disadvantage of the method is that the solution must be completed by taking into account slowly damped edge disturbances from the traverses, except for extremely long shells (compare ref. [14]).

The method used in the present paper belongs to a third group, where forces and displacements are also represented by a single Fourier series, but with trigonometric functions longitudinally and damped trigonometric functions circumferentially. According to KOEPCKE [11] this method was used first in 1936 by RABICH in a paper which has not been published. RABICH considered shells reinforced by ring ribs and with a load acting on a rib. Edge disturbances from the load generatrix were calculated using Finsterwalder's theory. AAS-JAKOBSEN [16, 17] used a similar approach, but solved the edge disturbance problem by his own iteration method. ODQUIST [18] considered short line loads along a generatrix of an isotropic shell and used Schorer's theory for analyzing the edge disturbances. The effect of line loads was investigated in the same manner by HOFF, KEMPNER and POHLE [19] and by KEMPNER, SHENG and POHLE [20], with the exception that these authors calculated the edge disturbances from Donnell's theory. Forces and displacements caused by radial and tangential line loads were also given by the writer [23] as special cases of a more general treatment of edge disturbances. The theory applied in [23] contained first order corrections to Donnell's theory.

In the present paper influence surfaces for isotropic shells are calculated by developing a concentrated load in a Fourier series in the direction of the generatrix. The analysis of the edge disturbances caused by each term in the load series is based on Donnell's theory and differs only formally from the one used in references [19] and [20].

The application of Donnell's theory implies a slight inaccuracy for long shells. However, it has the pronounced advantage of giving expressions for forces and displacements which depend on one parameter only, except for a multiplier to each quantity.

Fourier Series for a Concentrated Load

Let a simply supported shell of length l and radius r be subject to a concentrated radial unit load $P=1$ acting at a point with coordinates $\varphi=0$ and $x=x_0$ (Fig. 1). This load may be considered a delta-function of x

$$P = \delta(x-x_0). \tag{1}$$

This delta-function has the following properties

$$\delta(x-x_0) = 0 \quad \text{for } x \neq x_0,$$
$$\delta(x-x_0) = \infty \quad \text{for } x = x_0,$$
$$\int_{x_0-\epsilon}^{x_0+\epsilon} \delta(x-x_0)\,dx = 1 \text{ for any value of } \epsilon.$$

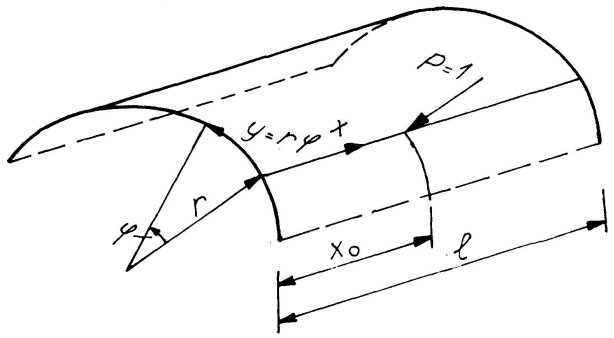

Fig. 1. Simply Supported Shell Loaded by a Concentrated Radial Load.

The load may be expanded in a sine series

$$P = \sum_{n=1}^{\infty} c_n \sin\frac{n\pi x}{l}, \tag{2}$$

where the coefficient c_n is

$$c_n = \frac{2}{l}\int_0^l P \sin\frac{n\pi x}{l}\,dx = \frac{2}{l}\sin\frac{n\pi x_0}{l}.$$

Hence

$$P = \delta(x-x_0) = \frac{2}{l}\sum_{n=1}^{\infty} \sin\frac{n\pi x_0}{l}\sin\frac{n\pi x}{l}. \tag{3}$$

Fourier Series for the Bending Moments

The stress resultants from each term of the series (3) may be calculated by the known methods for a simply supported shell. In the present paper the Donnell theory will be used for this purpose. Comments on the accuracy of this theory are given later. When influences from other edges are left out, the edge conditions along the loaded generatrix are:

shear force $N_{x\varphi} = 0$,
displacement in the direction of the arc $v = 0$,
angular rotation in the direction of the arc $\vartheta_\varphi = 0$,
transverse edge force $R_\varphi = -\frac{1}{2}\delta(x-x_0)$,
when the part of the shell which corresponds to a positive value of φ is considered.

Hence, the general term in a sine series for the transverse edge force is

$$R_{\varphi,n} = -\frac{1}{l}\sin\frac{n\pi x_0}{l}\sin\frac{n\pi x}{l}. \tag{4}$$

In the usual Fourier analysis for simply supported shells, the general series term for an arbitrary quantity caused by an edge disturbance may be written (compare [22])

$$H = [H]\,\mathrm{R}\{C_1\hat{H}_1 e^{m_1\varphi} + C_2\hat{H}_2 e^{m_2\varphi}\}. \tag{5}$$

In Eq. (5) influences from secondary edges are neglected. C_1 and C_2 are complex constants of integration. m_1 and m_2 are the roots of the characteristic equation

$$m_1 = \rho(-\alpha_1 + i\beta_1), \quad m_2 = \rho(-\alpha_2 + i\beta_2), \tag{6}$$

where

$$\begin{aligned}
\alpha_1 &= 2^{-1/2}[\{1+(1+\kappa)^2\}^{1/2} + (1+\kappa)]^{1/2},\\
\beta_1 &= 2^{-1/2}[\{1+(1+\kappa)^2\}^{1/2} - (1+\kappa)]^{1/2},\\
\alpha_2 &= 2^{-1/2}[\{1+(1-\kappa)^2\}^{1/2} - (1-\kappa)]^{1/2},\\
\beta_2 &= 2^{-1/2}[\{1+(1-\kappa)^2\}^{1/2} + (1-\kappa)]^{1/2}.
\end{aligned} \tag{7}$$

κ and ρ are the shell parameters

$$\begin{aligned}
\kappa &= \frac{n\pi}{\sqrt[4]{3(1-\nu^2)}}\frac{\sqrt{rh}}{l},\\
\rho &= \sqrt{n\pi}\sqrt[8]{3(1-\nu^2)}\sqrt{\frac{r}{l}}\sqrt[4]{\frac{r}{h}}.
\end{aligned} \tag{8}$$

$\mathrm{R}\{z\}$ means the real part of a complex number z.

The quantities $[H]$, $\hat{H}_1$ and $\hat{H}_2$ are given in Table 1 for the quantities occurring in the edge conditions mentioned above, and for the bending moments M_φ and M_x (for the development see for instance ref. [23] or [24]).

Table 1. $[H]$, $\hat{H}_1$ *and* $\hat{H}_2$

H	$[H]$	$\hat{H}_1$	$\hat{H}_2$
v	$\frac{r}{Eh\rho\kappa^2}\sin\frac{n\pi x}{l}$	$-\hat{m}_1\{1+i[1-(1+\nu)\kappa]\}$	$\hat{m}_2\{1-i[1+(1+\nu)\kappa]\}$
ϑ_φ	$\frac{2\rho}{Eh\kappa^2}\sin\frac{n\pi x}{l}$	$\hat{m}_1$	$\hat{m}_2$
$N_{x\varphi}$	$\frac{1}{\sqrt{\kappa}}\cos\frac{n\pi x}{l}$	$\hat{m}_1 i$	$-\hat{m}_2 i$
R_φ	$\frac{1}{2\rho}\sin\frac{n\pi x}{l}$	$\hat{m}_1\{1-(1-\nu)\kappa-i\}$	$-\hat{m}_2\{1+(1-\nu)\kappa+i\}$
M_x	$\frac{r}{2\rho^2}\sin\frac{n\pi x}{l}$	$-\kappa+(1+\kappa)\nu-\nu i$	$-\kappa-(1-\kappa)\nu-\nu i$
M_φ	$\frac{r}{2\rho^2}\sin\frac{n\pi x}{l}$	$1+(1-\nu)\kappa-i$	$-1+(1-\nu)\kappa-i$

$\hat{m}_1$ and $\hat{m}_2$ are the reduced roots

$$\hat{m}_1 = \frac{m_1}{\rho}, \qquad \hat{m}_2 = \frac{m_2}{\rho}. \tag{9}$$

Since $\varphi = 0$ at the edge considered, Eq. (5) gives the edge quantity

$$H_0 = [H]\,\mathrm{R}\{C_1 \hat{H}_1 + C_2 \hat{H}_2\}. \tag{10}$$

Let $$C_1 \hat{m}_1 = A_1 + i\,B_1, \qquad C_2 \hat{m}_2 = A_2 + i\,B_2.$$

Then the edge conditions

$$v = \vartheta_\varphi = N_{x\varphi} = 0, \qquad R_\varphi = -\frac{1}{l}\sin\frac{n\pi x_0}{l}\sin\frac{n\pi x}{l}$$

give the following 4 equations

$$\begin{aligned}
-A_1 + B_1[1-(1+\nu)\kappa] + A_2 + B_2[1+(1+\nu)\kappa] &= 0,\\
A_1 \qquad\qquad + A_2 \qquad\qquad &= 0,\\
-B_1 \qquad\qquad + B_2 &= 0,\\
A_1[1-(1-\nu)\kappa] + B_1 - A_2[1+(1-\nu)\kappa] + B_2 &= -\frac{2\rho}{l}\sin\frac{n\pi x_0}{l},
\end{aligned} \tag{11}$$

from which $$A_1 = B_1 = -A_2 = B_2 = -\frac{\rho}{2l}\sin\frac{n\pi x_0}{l}. \tag{12}$$

The constants of integration being known, the bending moments may be determined. On substituting the proper values from Table 1 and Eq. (12), one obtains the general series terms for the bending moments from Eq. (5), for $\nu = 0$

$$M_{x,n} = \frac{\kappa r}{4\rho l}\sin\frac{n\pi x_0}{l}\sin\frac{n\pi x}{l}\,\mathrm{R}\left\{\frac{1+i}{\hat{m}_1}e^{m_1\varphi} - \frac{1-i}{\hat{m}_2}e^{m_2\varphi}\right\}, \tag{13}$$

$$M_{\varphi,n} = -\frac{r}{4\rho l}\sin\frac{n\pi x_0}{l}\sin\frac{n\pi x}{l}\,\mathrm{R}\left\{\frac{1+i}{\hat{m}_1}(1+\kappa-i)\,e^{m_1\varphi} + \frac{1-i}{\hat{m}_2}(1-\kappa+i)\,e^{m_2\varphi}\right\}. \tag{14}$$

For a value of Poisson's ratio different from zero the moments are obtained from

$$\begin{aligned}
M_{\varphi,\nu} &= M_{\varphi,\nu=0} + \nu\,M_{x,\nu=0},\\
M_{x,\nu} &= M_{x,\nu=0} + \nu\,M_{\varphi,\nu=0}
\end{aligned} \tag{15}$$

(the relations are exact only when the actual value of ν is used for calculating κ and ρ).

Eqs. (13) and (14) are transformed into real form by introducing

$$e^{m_1\varphi} = e^{(-\alpha_1+i\beta_1)\rho\varphi} = e^{-\alpha_1\rho\varphi}(\cos\beta_1\rho\varphi + i\sin\beta_1\rho\varphi) = f_2 + i\,f_1, \tag{16}$$

$$e^{m_2\varphi} = e^{(-\alpha_2+i\beta_2)\rho\varphi} = e^{-\alpha_2\rho\varphi}(\cos\beta_2\rho\varphi + i\sin\beta_2\rho\varphi) = f_4 + i\,f_3, \tag{17}$$

which gives

$$M_x = \sum_{n=1,2,3\ldots} \frac{1}{2n\pi} \sin\frac{n\pi x_0}{l} \sin\frac{n\pi x}{l} \frac{1}{2}\kappa\sqrt{\kappa}\{(\alpha_1^*+\beta_1^*)f_1-(\alpha_1^*-\beta_1^*)f_2 + (\alpha_2^*-\beta_2^*)f_3+(\alpha_2^*+\beta_2^*)f_4\}, \tag{18}$$

$$M_\varphi = \sum_{n=1,2,3\ldots} \frac{1}{2n\pi} \sin\frac{n\pi x_0}{l} \sin\frac{n\pi x}{l} \frac{1}{2}\kappa\sqrt{\kappa}\left\{-\left[\alpha_1^*+\left(1+\frac{2}{\kappa}\right)\beta_1^*\right]f_1 + \left[\left(1+\frac{2}{\kappa}\right)\alpha_1^*-\beta_1^*\right]f_2-\left[\alpha_2^*-\left(1-\frac{2}{\kappa}\right)\beta_2^*\right]f_3-\left[\left(1-\frac{2}{\kappa}\right)\alpha_2^*+\beta_2^*\right]f_4\right\} \tag{19}$$

and

$$M_x+M_\varphi = \sum_{n=1,2,3\ldots} \frac{1}{2n\pi} \sin\frac{n\pi x_0}{l} \sin\frac{n\pi x}{l}\sqrt{\kappa}\,(-\beta_1^* f_1+\alpha_1^* f_2-\beta_2^* f_3+\alpha_2^* f_4), \tag{20}$$

where

$$\alpha_1^* = \frac{\alpha_1}{\alpha_1^2+\beta_1^2}, \qquad \beta_1^* = \frac{\beta_1}{\alpha_1^2+\beta_1^2}, \qquad \alpha_2^* = \frac{\alpha_2}{\alpha_2^2+\beta_2^2}, \qquad \beta_2^* = \frac{\beta_2}{\alpha_2^2+\beta_2^2}. \tag{21}$$

The equations (18) and (19) give the moments at an arbitrarily chosen point (x,φ), caused by a unit load at the point $(x_0,0)$. The moment found at (x,φ), however, is equal to the moment at $(x_0,0)$ caused by a unit load at (x,φ). In other words, the function resulting constitutes the influence surface for the bending moments at $(x_0,0)$.

As was mentioned previously, influences from other edges were left out in the analysis outlined above. Strictly speaking, the influence functions (18) and (19) are thus only valid for shells extending to infinity in the circumferential direction. Except for points near the edge, the influence from other straight edges are of little importance. In all cases such disturbances may be described by one or a few Fourier terms and may be calculated by known methods.

Improvement of Convergence, Numerical Work

Since the bending moment at $(x_0,0)$ will be infinite when the load is placed at the same point, $(x_0,0)$ is a singular point in the influence surface. This singularity makes the series (18)—(20) converge slowly in points near the load generatrix.

In the numerical computations which follows, influence surfaces for the point $x_0=l/2$ only will be considered. The slowest convergence occurs along the generatrix $\varphi=0$. Along this generatrix the bending moments obtained from Eqs. (18) and (20) are

$$M_x = \frac{1}{2\pi} \sum_{n=1,3,5\ldots} (-1)^{\frac{n-1}{2}} \frac{1}{n} \sin\left(n\pi\frac{x}{l}\right) \frac{\kappa}{2} \sqrt{\kappa}\,(-\alpha_1^* + \beta_1^* + \alpha_2^* + \beta_2^*), \tag{22}$$

$$M_x + M_\varphi = \frac{1}{\pi} \sum_{n=1,3,5\ldots} (-1)^{\frac{n-1}{2}} \frac{1}{n} \sin\left(n\pi\frac{x}{l}\right) \frac{\sqrt{\kappa}}{2} (\alpha_1^* + \alpha_2^*), \tag{23}$$

where the expressions

$$\frac{\kappa}{2}\sqrt{\kappa}\,(-\alpha_1^* + \beta_1^* + \alpha_2^* + \beta_2^*)$$

and

$$\frac{\sqrt{\kappa}}{2}(\alpha_1^* + \alpha_2^*)$$

approach 1 when n increases. Hence, the convergence of the series (22) and (23) may be improved by subtracting the series

$$\sum_{n=1,3,5\ldots} (-1)^{\frac{n-1}{2}} \frac{1}{n} \sin\left(n\pi\frac{x}{l}\right) = -\frac{1}{2} \ln \frac{\cos\pi\frac{x}{l}}{1+\sin\pi\frac{x}{l}}. \tag{24}$$

Eqs. (22) and (23) are then replaced by

$$M_x = -\frac{1}{4\pi} \ln \frac{\cos\pi\frac{x}{l}}{1+\sin\pi\frac{x}{l}} + \frac{1}{2\pi} \sum_{n=1,3,5\ldots} (-1)^{\frac{n-1}{2}} \frac{1}{n} \sin\left(n\pi\frac{x}{l}\right) \cdot \left[\frac{\kappa}{2}\sqrt{\kappa}\,(-\alpha_1^* + \beta_1^* + \alpha_2^* + \beta_2^*) - 1\right], \tag{25}$$

$$M_x + M_\varphi = -\frac{1}{2\pi} \ln \frac{\cos\pi\frac{x}{l}}{1+\sin\pi\frac{x}{l}} + \frac{1}{\pi} \sum_{n=1,3,5\ldots} (-1)^{\frac{n-1}{2}} \frac{1}{n} \sin\left(n\pi\frac{x}{l}\right) \cdot \left[\frac{\sqrt{\kappa}}{2}(\alpha_1^* + \alpha_2^*) - 1\right]. \tag{26}$$

The diagrams which follow have been computed from Eqs. (25) and (26) for $\varphi = 0$, and from Eqs. (18) and (20) for $\varphi \neq 0$. The shape of the influence surfaces depends on a parameter characterizing the dimensions of the shell

$$\delta = \frac{l}{\sqrt{rh}}.$$

The parameters occurring in the series may be expressed by δ (compare Eqs. (8) and (16)) as follows

$$\kappa = \frac{n\pi}{\sqrt[4]{3(1-\nu^2)}} \frac{\sqrt{rh}}{l} = \frac{n\pi}{\sqrt[4]{3(1-\nu^2)}}\delta,$$

$$\rho\varphi = \sqrt{n\pi}\sqrt[8]{3(1-\nu^2)}\,\sqrt{\frac{r}{l}}\sqrt[4]{\frac{r}{h}\frac{y}{r}} = \sqrt{n\pi}\sqrt[8]{3(1-\nu^2)}\,\sqrt{\delta}\,\frac{y}{l}. \tag{27}$$

The moments have been calculated for

$$\frac{x}{l} = \quad 0.1, \quad 0.2, \quad 0.3, \quad 0.4, \quad 0.45, \quad 0.5$$

$$\frac{y}{l} = \; 0, \; 0.1, \quad 0.2, \quad 0.3, \quad 0.4, \quad 0.45, \quad 0.5$$

For $y/l = 0$ the series diverge in the point $x/l = 0.5$, which in this case has been replaced by $x/l = 0.48$. Between the points thus obtained the equidistant curves in the diagrams have been drawn by curvilinear interpolation.

The value of Poisson's ratio occurring in Eqs. (27) is of no actual importance. In the numerical computations it has been put equal to 0.2.

The calculations outlined were programmed by the Mathematics Group at the Norwegian Defence Research Establishment and carried out at their Ferranti Mercury computer.

Figs. 3—7 and 9—13 show the resulting influence diagrams for various values of the parameter $\delta = l/\sqrt{rh}$ from $\delta = 1$ to $\delta = 25$. For comparison, the case $\delta = 0$ (plane plate) is shown in Figs. 2 and 8. These diagrams are based on those of PUCHER [1]. $\delta = 1$ corresponds to a very slight curvature, and the diagrams show no substantial difference from $\delta = 0$.

As the curvature increases the area of positive influence coefficients near the load is diminished. This is particularly the case for M_x and to a lesser degree for M_φ.

The diagrams show furthermore that loads outside the zero curve surrounding the point considered give only small moments in this point.

Hence, if the curvature is not too small, the bending moments under a load distributed over a small area is a local effect which is little influenced by edge effects or other loads. For this reason the diagrams presented may be used for calculating the bending moments under a concentrated load in any place on the shell, if only not too near the edge. For such a purpose, a representation showing less difference between the various values of δ would have been preferable. At the same time a higher degree of accuracy is desirable for the high values of δ. This may be obtained by choosing as variables for instance

for M_x: $$\delta\frac{x}{l} = \frac{x}{\sqrt{rh}} \quad \text{and} \quad \delta\frac{y}{l} = \frac{y}{\sqrt{rh}},$$

for M_φ: $$\frac{x}{l} \quad \text{and} \quad \sqrt{\delta}\frac{y}{l} = \frac{y}{\sqrt{l}\sqrt{rh}}.$$

The writer intends to present, in a subsequent paper, diagrams in this form and tables for moments under loads covering small areas.

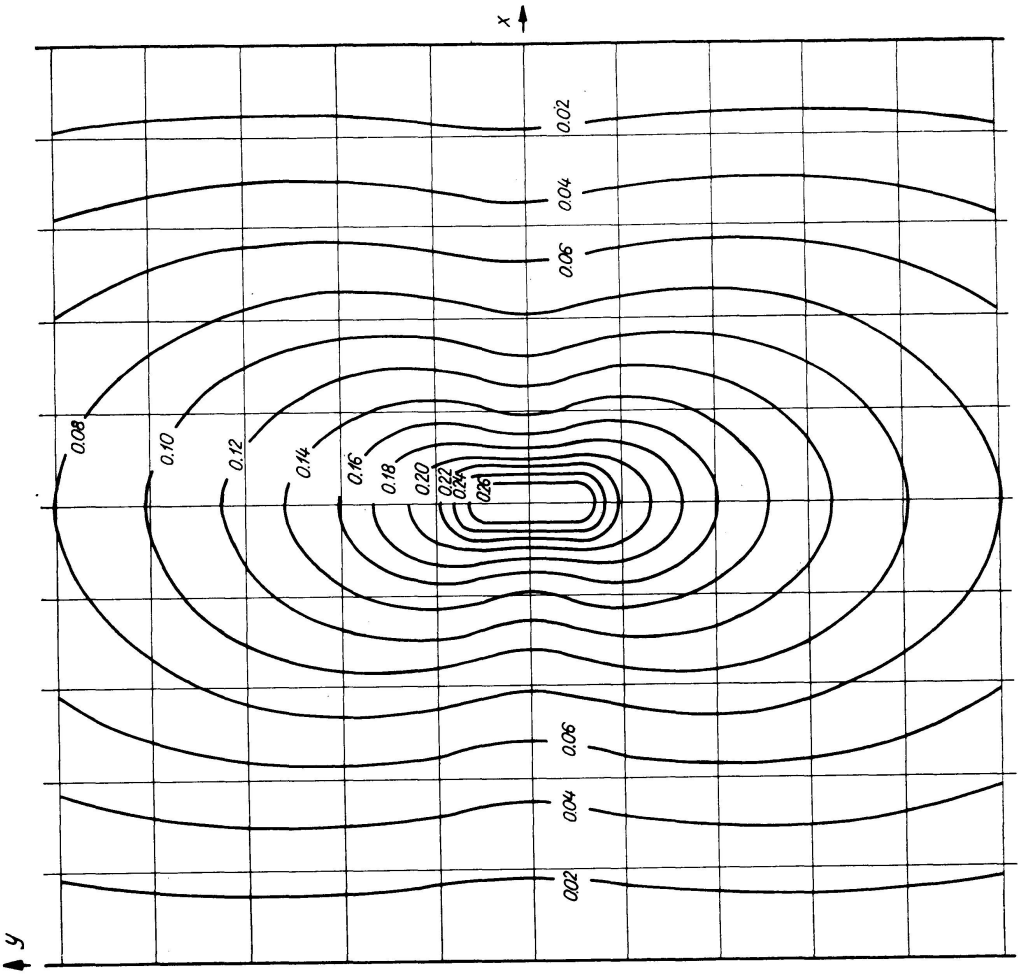

Fig. 3. Influence Surface for M_x for $l/\sqrt{rh}=1$.

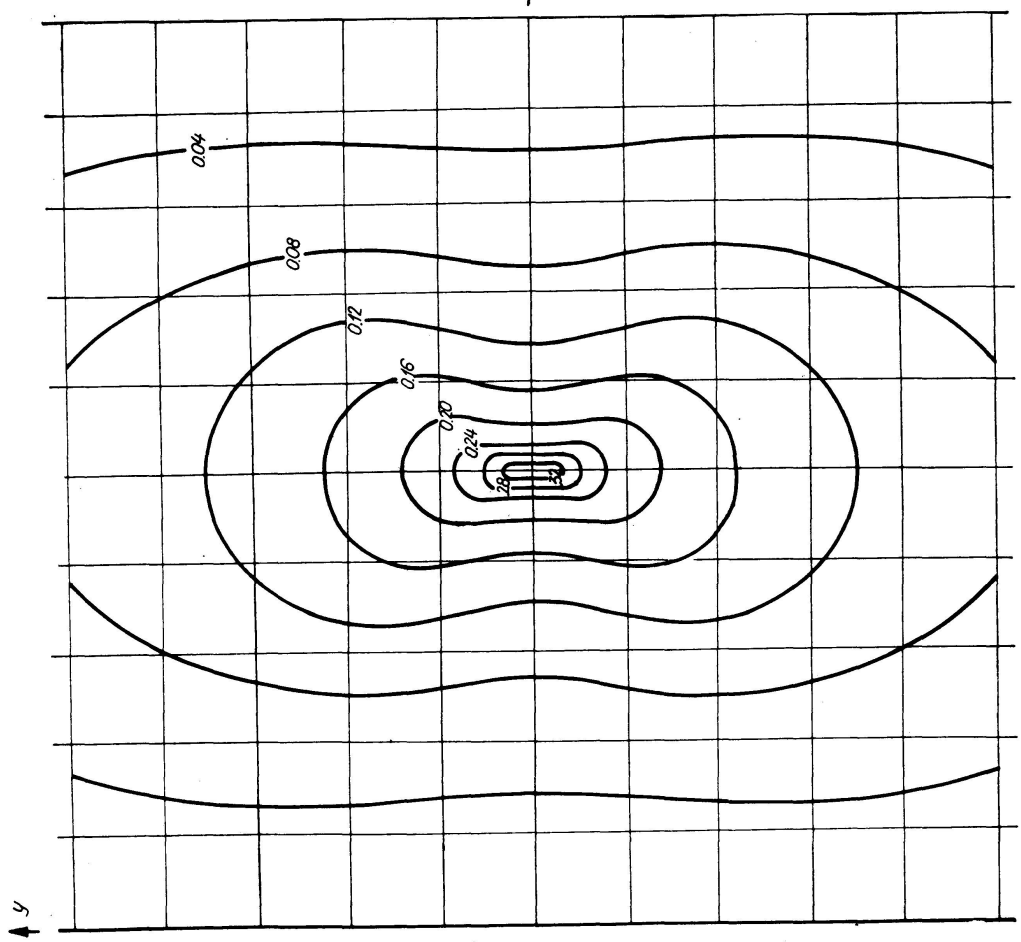

Fig. 2. Influence Surface for M_x for $l/\sqrt{rh}=0$.

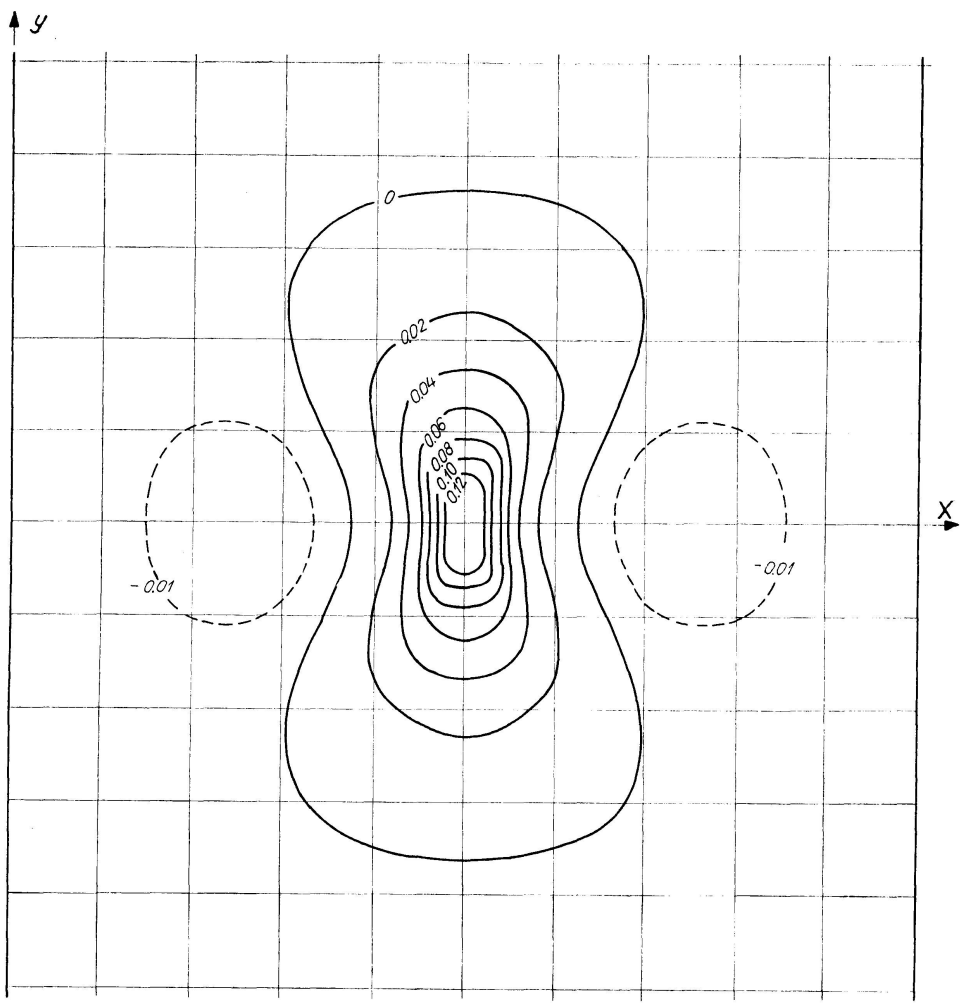

Fig. 4. Influence Surface for M_x for $l/\sqrt{rh}=5$.

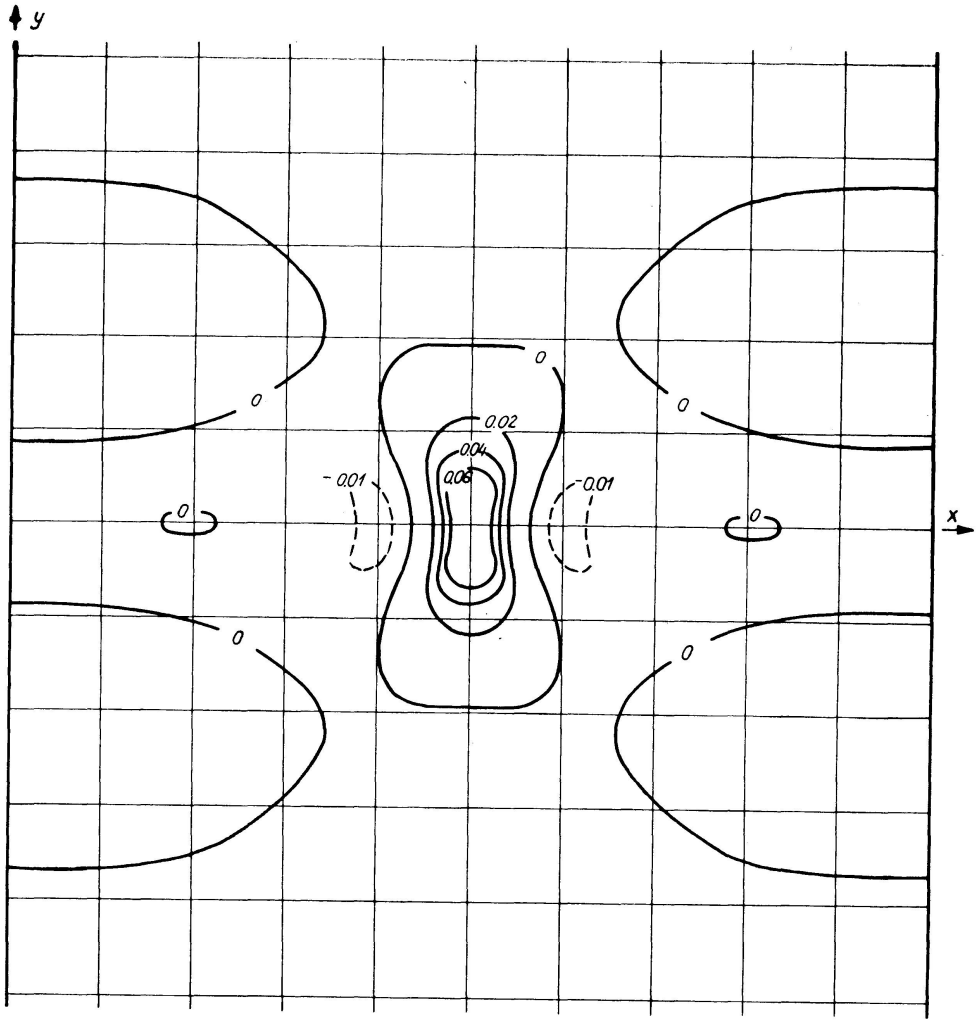

Fig. 5. Influence Surface for M_x for $l/\sqrt{rh}=10$.

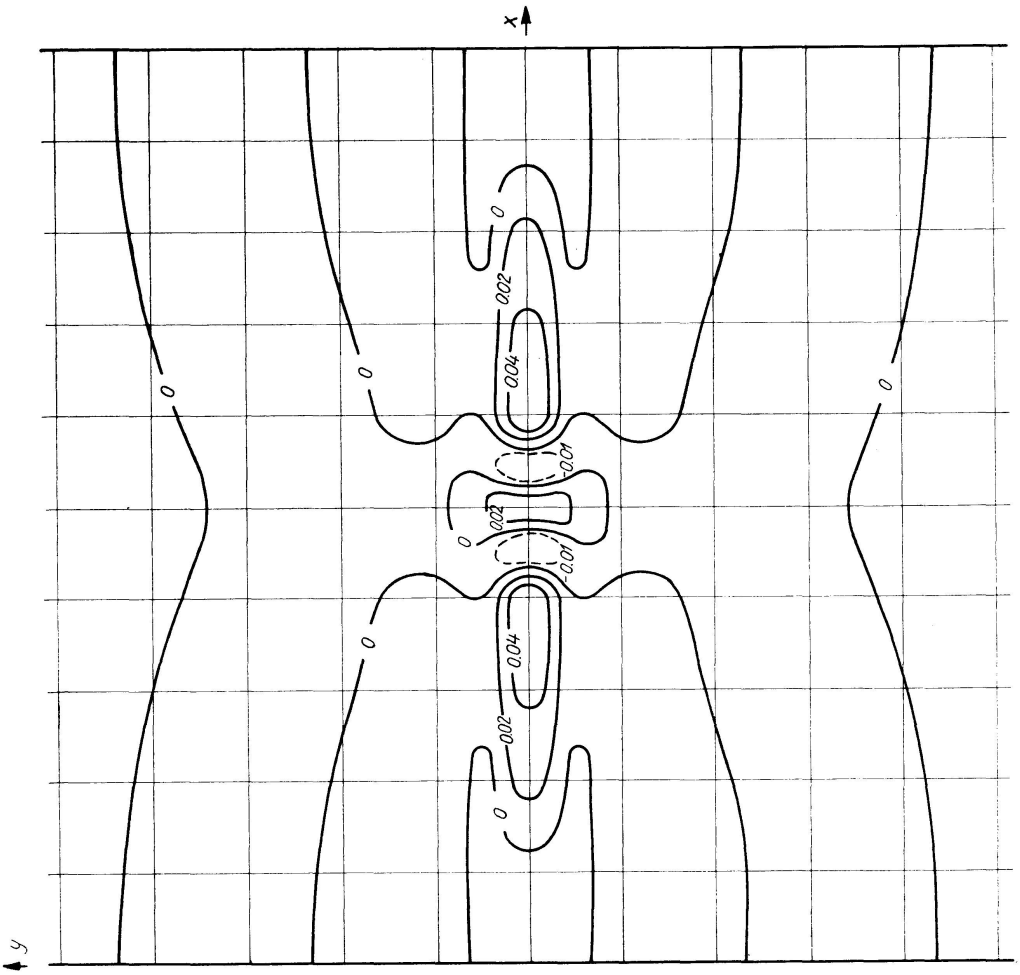

Fig. 7. Influence Surface for M_x for $l/\sqrt{rh}=25$.

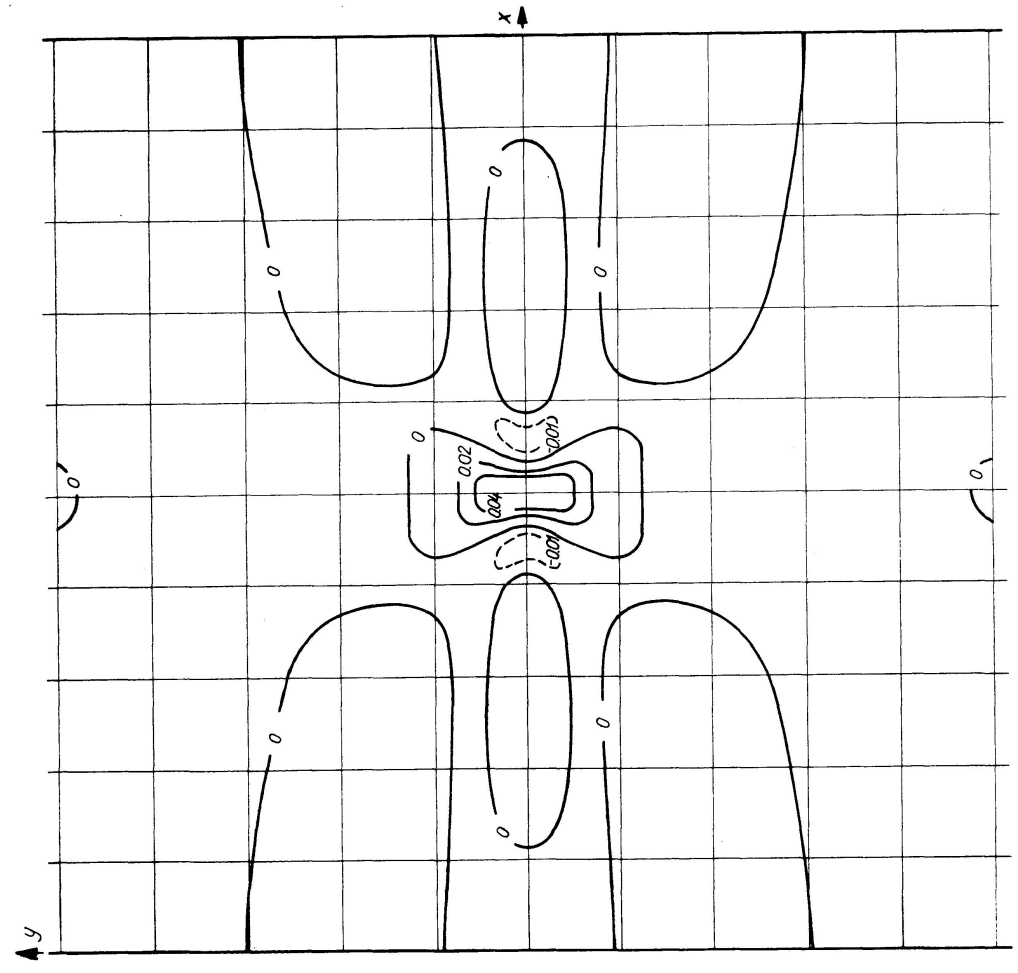

Fig. 6. Influence Surface for M_x for $l/\sqrt{rh}=15$.

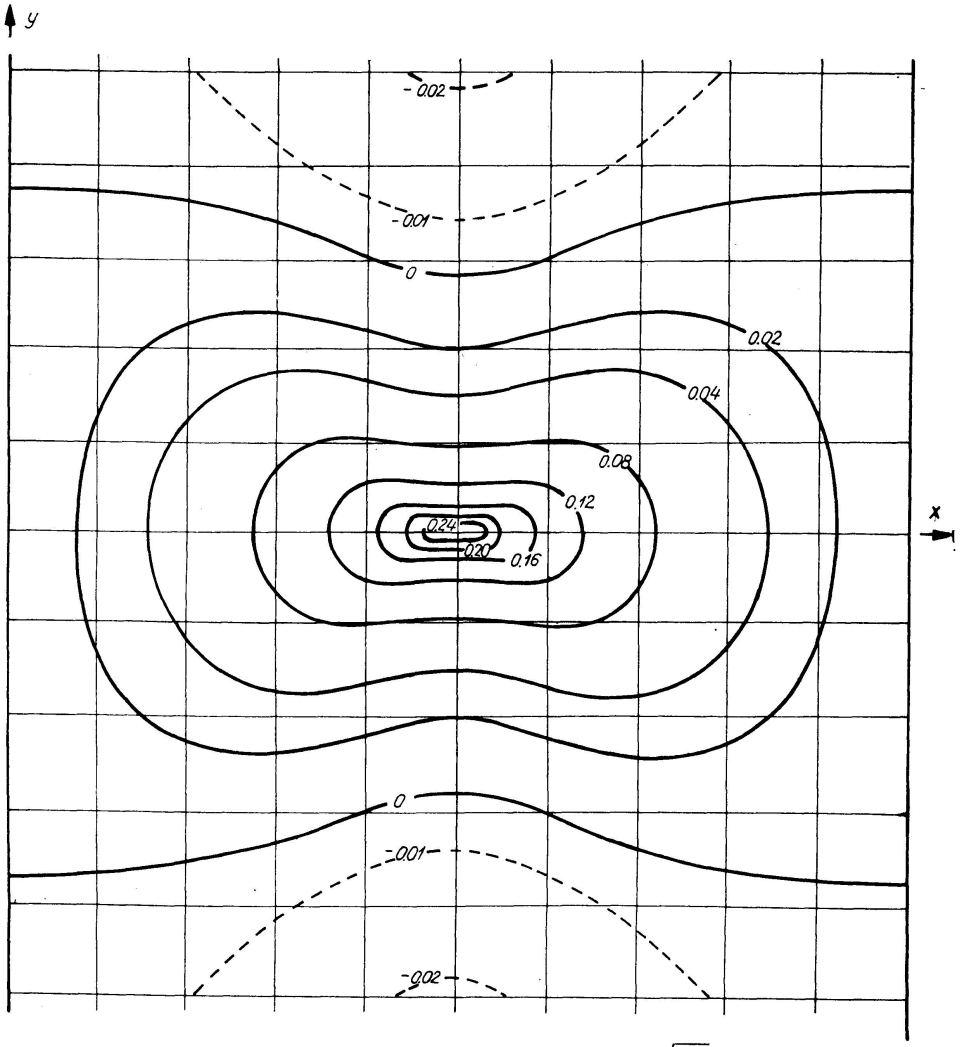

Fig. 8. Influence Surface for M_y for $l/\sqrt{rh}=0$.

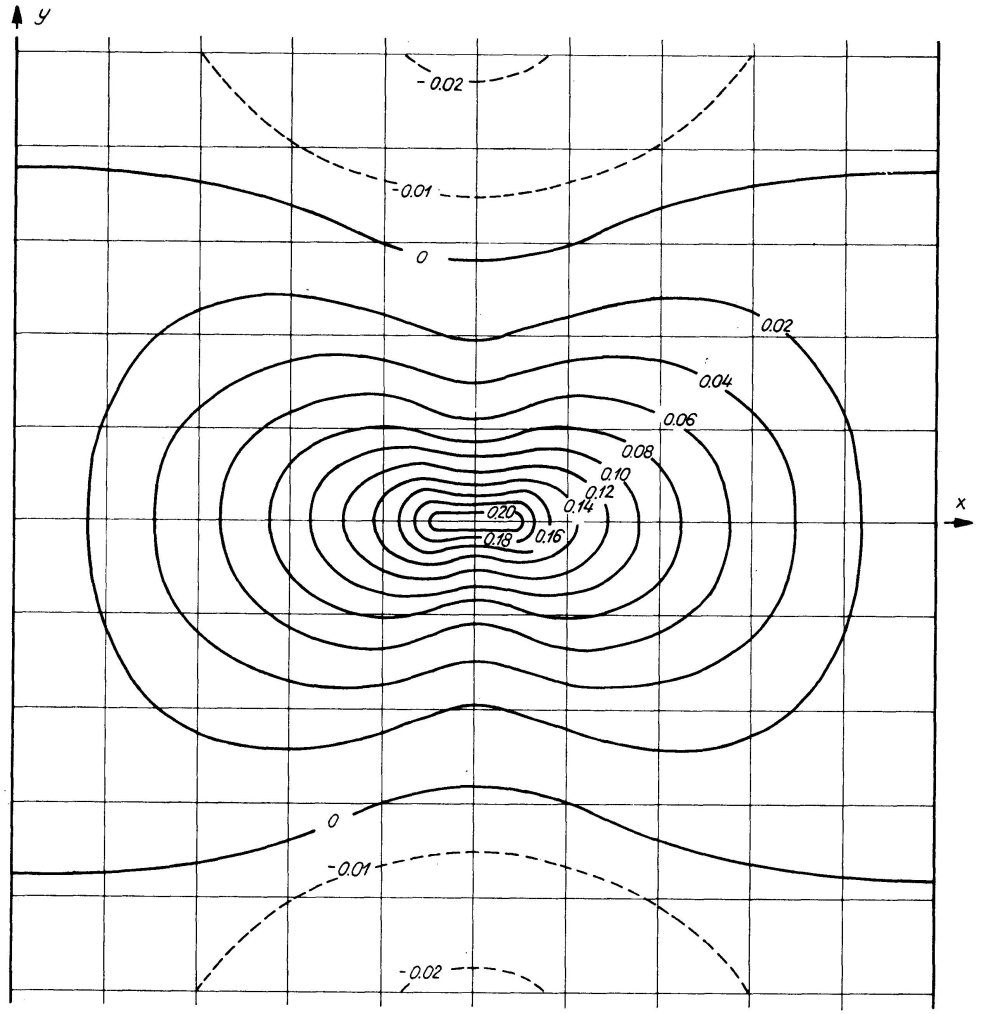

Fig. 9. Influence Surface for M_y for $l/\sqrt{rh}=1$.

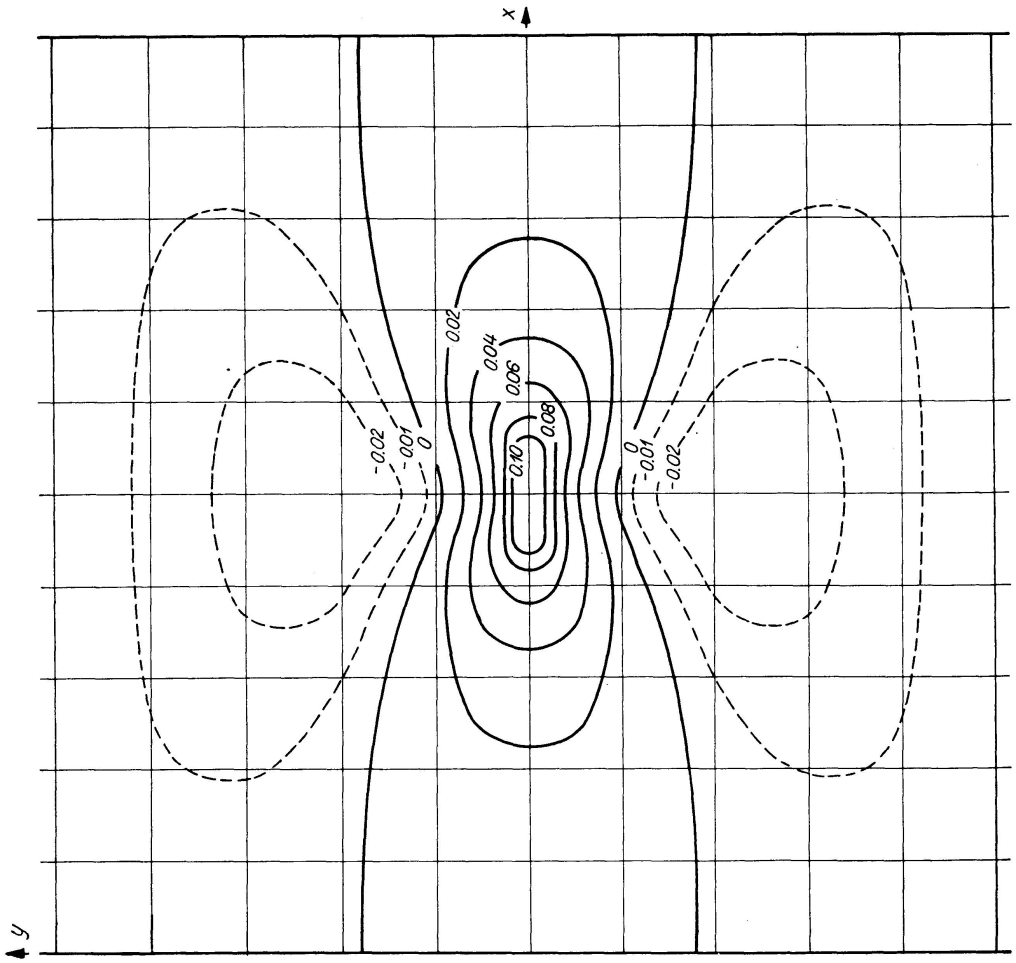

Fig. 11. Influence Surface for M_y for $l/\sqrt{rh}=10$.

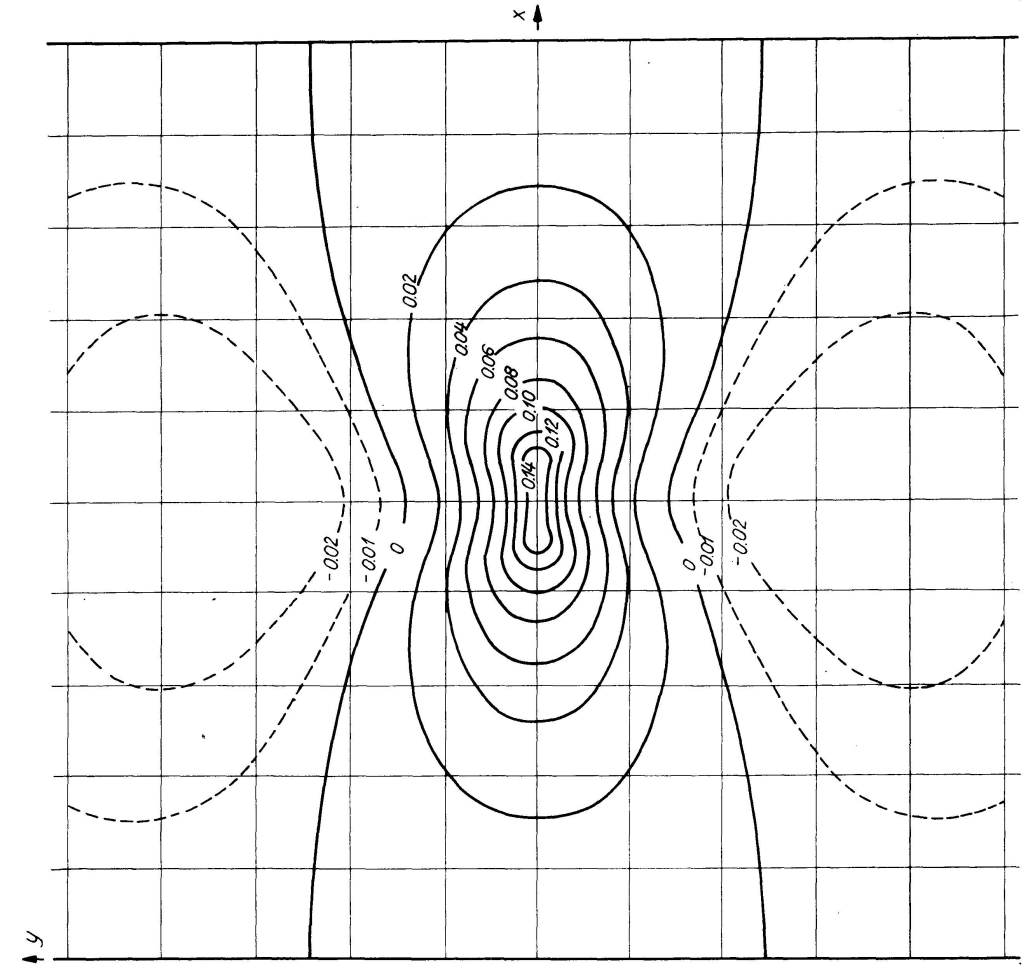

Fig. 10. Influence Surface for M_y for $l/\sqrt{rh}=5$.

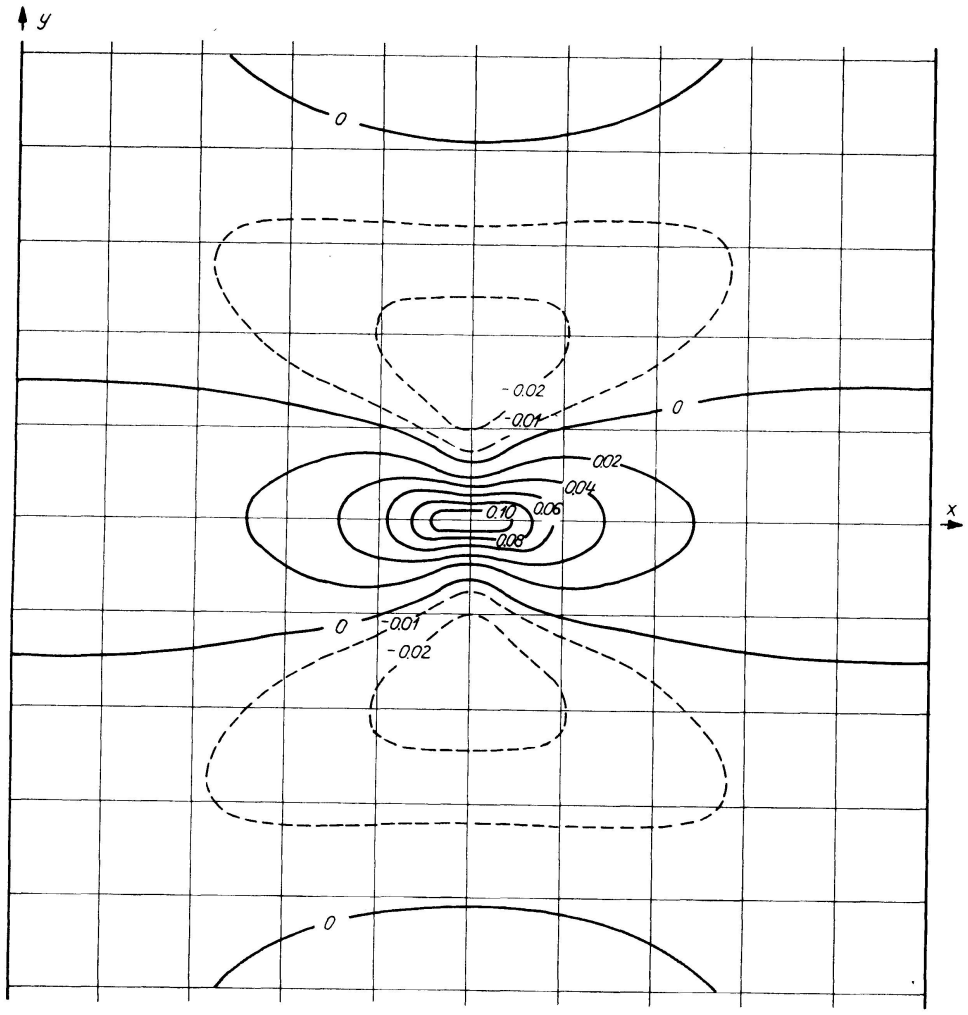

Fig. 12. Influence Surface for M_y for $l/\sqrt{rh}=15$.

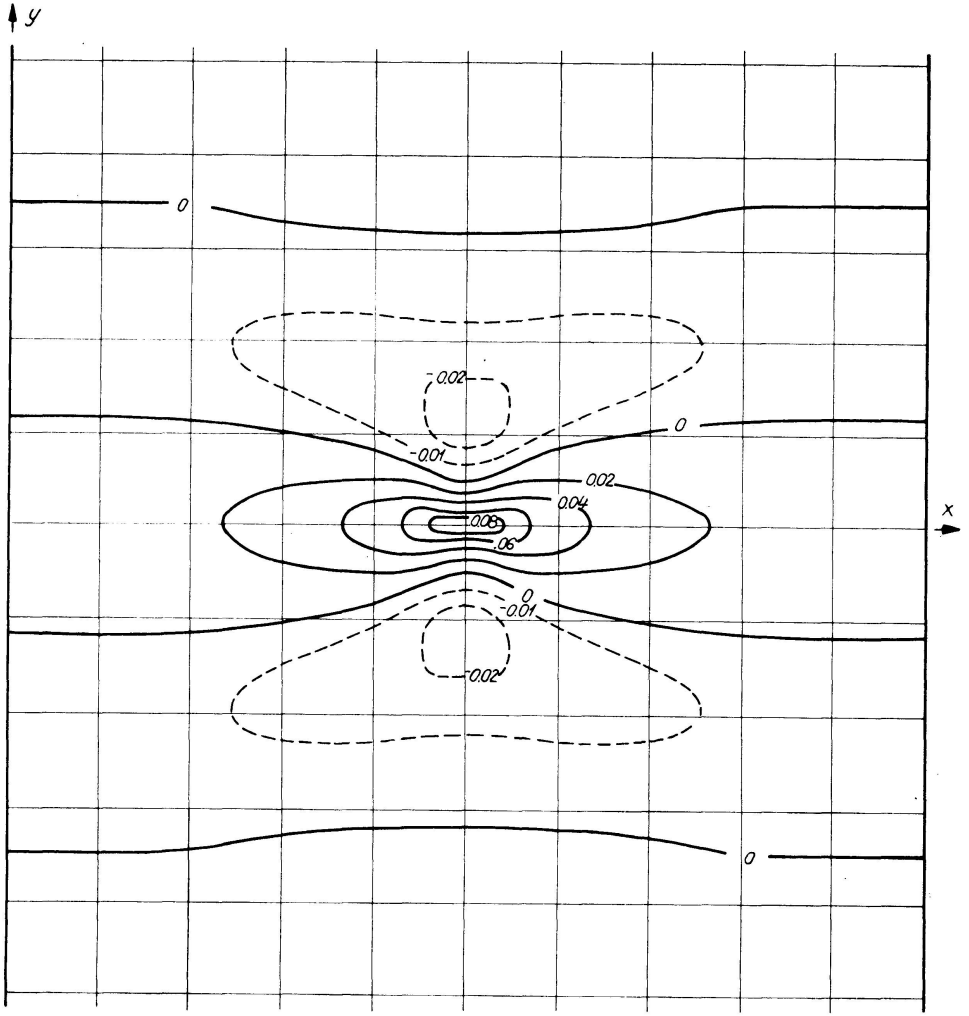

Fig. 13. Influence Surface for M_y for $l/\sqrt{rh}=25$.

Comments on the Accuracy of the Solution

In reference [23], pp. 95 and 83, expressions are given for bending moments caused by a sine-shaped line load. The expressions are deduced from a "New approximate" theory containing correction terms to the Donnell theory. For the case of a concentrated load these expressions give for $\varphi = 0$ and $\nu = 0$

$$M_x = \frac{1}{2\pi} \sum_{n=1,3,5\ldots} (-1)^{\frac{n-1}{2}} \frac{1}{n} \sin\left(n\pi \frac{x}{l}\right) \frac{\kappa}{2} \sqrt{\kappa}\,(-\alpha_1^* + \beta_1^* + \alpha_2^* + \beta_2^*), \tag{28}$$

$$M_x + M_\varphi = \frac{1}{\pi} \sum_{n=1,3,5\ldots} (-1)^{\frac{n-1}{2}} \frac{1}{n} \sin\left(n\pi \frac{x}{l}\right) \frac{\sqrt{\kappa}}{2} \left[\alpha_1^* + \alpha_2^* + \frac{1}{2\rho^2}(-\alpha_1^* + \beta_1^* + \beta_2^* + \alpha_2^*)\right]. \tag{29}$$

where ρ is defined in Eq. (8). In addition κ should be replaced by $\kappa - \frac{1}{2\rho^2}$ in Eqs. (7) when calculating α_1, β_1, α_2 and β_2, from which α_1^*, β_1^*, α_2^* and β_2^* are calculated by use of Eqs. (21).

For a normally long concrete shell roof one may take $l = 2{,}5\,r$, $r = 100\,h$ which gives (compare Eqs. (8)) $\rho^2 \approx 16\,n$, $\kappa \approx 0.10\,n$.

Formulas (28) and (29) for these values of the parameters give differences from the results obtained from Donnell's theory (Eqs. (22) and (23)) of the magnitude

$$0.001 \quad \text{in } M_\varphi,$$
$$0.0001 \text{ in } M_x.$$

Thus, the errors are of no importance for engineering purposes, even in the case of shells of this length.

Notations

r	shell radius
l	shell length (span)
x	coordinate measured axially from end of span
x_0	value of x at the load point
$y, \varphi = y/r$	coordinates measured along the arc
P	concentrated load
$\delta(x - x_0)$	δ-function
c_n	coefficient of the general term in a Fourier series
$N_{x\varphi}$	shear force
R_φ	transverse edge force
M_x	bending moment in x-direction
M_φ	bending moment in φ-direction

v	displacement in φ-direction
ϑ_φ	angular rotation of an arc
$N_{x\varphi,n}$ etc.	the general term in the Fourier series for the corresponding quantity
H	arbitrary force or displacement
$[H]$	multiplier of H
$\hat{H}_1, \hat{H}_2$	characteristic coefficients of H
$\mathrm{R}\{z\}$	real part of a complex number z
i	imaginary unit
E	modulus of elasticity
ν	Poisson's ratio
κ, ρ, δ	nondimensional shell parameters
m_1, m_2	roots of the characteristic equation
$\hat{m}_1, \hat{m}_2$	reduced values of m_1 and m_2
$\alpha_1, \beta_1, \alpha_2, \beta_2$	real and imaginary parts of $\hat{m}_1$ and $\hat{m}_2$
$\alpha_1^*, \alpha_1^*, \beta_2^*, \beta_2^*$	nondimensional quantities (see Eq. (21))
$A\,B\,C$	constants of integration

Acknowledgement

I wish to express my gratitude to the Mathematics Group of the Norwegian Defence Research Establishment for undertaking the work of programming and carrying out the computations of this paper, and to The Technical University of Norway Fund for bearing the computing expenses.

References

1. Pucher, A.: Einflußfelder elastischer Platten. 2. Aufl. Springer-Verlag, Wien 1958.
2. Hoeland, Günter: Stützmomenten-Einflußfelder durchlaufender Platten. Springer-Verlag, Berlin 1957.
3. Persen, Leif N.: Influence Fields for Circular and Infinite Cantilever Plates. Tekniske skrifter Nr. 1N. Teknisk Ukeblad, Oslo 1951.
4. Yuan, S. W.: Thin Cylindrical Shells Subjected to Concentrated Loads. Quarterly of Applied Mathematics Vol. IV, pp. 13—26, 1946.
5. Bieger, K. W.: Einflußflächen der Kreiszylinderschalen. Dissertation, Technische Universität Berlin 1959.
6. Reissner, H.: Formänderungen und Spannungen einer dünnwandigen, an den Rändern frei aufliegenden beliebig belasteten Zylinderschale. Zeitschrift für angewandte Mathematik und Mechanik. Bd. 13, p. 133, 1933.
7. Bijlaard, P. P.: Stresses from Radial Loads in Cylindrical Pressure Vessels. Welding Journal, Vol. 33, pp. 615s—623s, 1954.
8. Bijlaard, P. P.: Stresses from Local Loadings in Cylindrical Pressure Vessels. Trans. ASME Vol. 77, No. 6, pp. 805—814, 1955.

9. WLASSOW, W. S.: Allgemeine Schalentheorie und ihre Anwendung in der Technik. Akademie-Verlag, Berlin 1958 (translated edition).
10. ERNST, W.: Die Greenschen oder Einflußfunktionen des kreiszylindrischen Rohres. Arbeit zur Erlangung des Grades eines Dr.-Ing. habil. der Technischen Hochschule Berlin, Berlin 1943.
11. KOEPCKE, W.: Die Berechnung von Kreiszylinderschalen unter Flächen-, Linien- und Einzellasten. Habilitationsschrift, Techn. Universität Berlin-Charlottenburg 1949.
12. LUNDGREN, H.: Einzellasten auf Zylinderschalen mit Ringversteifungen. Bygningsstatiske Meddelelser, Aargang XIII, pp. 1—24, 1942.
13. YUAN, S. W. and TING, L.: On Radial Deflections of a Cylinder Subjected to Equal and Opposite Concentrated Radial Loads. J. App. Mech. 24, p. 278, 1957.
14. TING, L. and YUAN, S. W.: On Radial Deflection of a Cylinder of Finite Length with Various End Conditions. Journal of the Aeronautical Sciences, Vol. 25, pp. 230—234, 1958.
15. MORLEY, L. S. D.: The Thin-Walled Circular Cylinder Subjected to Concentrated Radial Loads. Quarterly Journal of Mechanics and Applied Mathematics. Vol. XIII, Part 1, pp. 24—37, 1960.
16. AAS-JAKOBSEN, A.: Einzellasten auf Kreiszylinderschalen. Der Bauingenieur, XXII. Jahrg., pp. 343—346, 1941.
17. AAS-JAKOBSEN, A.: Enkeltlaster på sylinderskall. Bygningsstatiske Meddelelser, Aargang 15, pp. 41—64, 1944.
18. ODQUIST, F. K. G.: Action of Forces and Moments Symmetrically Distributed Along a Generatrix of a Thin Cylindrical Shell. Journal of Applied Mechanics, Vol. 13, pp. A 106—A 108, 1946.
19. HOFF, N. J., KEMPNER, J. and POHLE, F. V.: Line Load Applied Along Generators of Thin-Walled Circular Cylindrical Shells of Finite Length. Quarterly of Applied Mathematics, Vol. XI, pp. 411—425, 1954.
20. KEMPNER, J., SHENG, J. and POHLE, F. V.: Tables and Curves for Deformations and Stresses in Circular Cylindrical Shells Under Localized Loadings. Journal of the Aeronautical Sciences. February 1957, pp. 119—129.
21. DONNELL, L. H.: Stability of Thin-Walled Tubes under Torsion. NACA Rep. No. 479, 1934.
22. LUNDGREN, H.: Cylindrical Shells. The Danish Technical Press. Copenhagen 1949.
23. HOLAND, I.: Design of Circular Cylindrical Shells. Oslo University Press, Oslo 1957.
24. HOLAND, I.: A Contribution to the Theory of Circular Cylindrical Shells. Proceedings of a Symposium on Concrete Shell Roof Construction, Teknisk Ukeblad, Oslo, 1958.

Summary

The paper presents influence surfaces for the bending moments in circular cylindrical shells of various curvatures.

The influence surfaces have been calculated in the following manner: A unit radial load is represented by a Fourier series in the axial direction. By use of the Donnell theory the bending moments corresponding to the general term in the load series are found as explicit expressions. The influences from other edges parallel to the axis are left out. Thus single Fourier series for the bending moments are established. They are evaluated numerically by an electronic computer.

Résumé

L'auteur présente des surfaces d'influence pour les moments de flexion des voiles cylindriques circulaires, en considérant différentes valeurs de la «courbure».

Ces surfaces ont été calculées de la façon suivante: Une charge unitaire radiale est représentée par une série de Fourier le long d'une génératrice. La théorie de Donnell permet d'écrire explicitement les moments de flexion correspondant au terme général des séries de charge. On néglige les influences provenant des autres lisières, parallèles à l'axe du voile. Ainsi les moments de flexion sont représentés par des séries simples, dont les valeurs sont déterminées à l'aide d'une calculatrice électronique.

Zusammenfassung

In dieser Abhandlung werden für verschiedene Krümmungswerte Momenteneinflußflächen von Kreiszylinderschalen vorgelegt.

Der Berechnungsgang ist der folgende: Eine radial wirkende Einheitslast wird in eine Fourierreihe längs der Mantellinie entwickelt. Mit Hilfe der Theorie von Donnell können die dem allgemeinen Glied der Belastungsreihe entsprechenden Biegungsmomente in expliziter Form angeschrieben werden. Die Einflüsse von andern parallel zur Schalenachse verlaufenden Rändern werden vernachlässigt. Auf diese Art und Weise werden die Biegungsmomente durch einfache Fourierreihen dargestellt. Diese werden dann von einer elektronischen Rechenmaschine numerisch ausgewertet.